Chapter 3
Morphology and Mechanics of the Young Minipig Cranium

Stephen Alexander, C. Allan Gunnarsson, Ann Mae DiLeonardi, and Tusit Weerasooriya

Abstract The Göttingen miniature pig is a useful surrogate to understand mechanisms of traumatic brain injury (TBI) in the human. However, the mechanical response of the minipig skull has not been previously reported. In this study, cranial samples were extracted from the skulls of adolescent minipigs (six months of age, average weight of 13.8 kg). The microstructure was first characterized using high-resolution μCT. A highly gradient structure was observed, with the bone volume fraction (BVF) almost doubling in the through-thickness (depth) dimension. These specimens were then mechanically loaded in quasi-static compression. The surface strain distribution along the loading direction was measured during the experiments using digital image correlation (DIC). Depth-dependent moduli were derived from the measured DIC strains rather than machine displacement, due to the large gradient in morphology. An elasticity-morphology relationship from literature was extended to represent the modulus variation in the functionally gradient skull structure (BVF), by calibrating the relationship with the experimentally derived local moduli. The model enables the prediction of local moduli based solely on the morphological parameter BVF measured with μCT, and also provided an estimation of the modulus of the bony phase of the cranium.

Keywords Cranial bone mechanical properties • Fabric tensor • Mean intercept length • Minipig skull morphology • Skull mechanics

3.1 Introduction

The Göttingen minipig is used as a surrogate in impact experiments designed to better understand the mechanisms by which mechanical loading induces traumatic brain injury (TBI). However, cranial mechanics and morphology must be understood in order to accurately scale any quantitative results, such as injury thresholds, from non-human TBI experiments to the human anatomy.

Both the mechanical response and the morphology of the skull have been previously studied for the human [1, 2] and large-breed pig [3]. Mature human cranial bone is a sandwich structure composed of three layers spanning the through-thickness axis, from the brain-most side of the skull to the skin-most side. The outer and inner tables are composed of dense cortical bone, while the middle layer, the diploë, is porous trabecular bone. On the other hand, studies have reported a random orientation of bone across the plane transverse to the through-thickness axis [4]. Importantly, skull morphology changes dramatically during maturation, developing from a single layer of dense bone [3].

However, the size and porosity of the minipig skull is known to differ significantly from that of larger breeds [5], requiring independent characterization. In this study, micro-computed tomography (μCT) was used to measure spatial variation in porosity and to quantify the orientation of the bone phase within the structure. Specimens were also loaded at a quasi-static rate in the through-thickness (depth) direction, normal to the outer surface of the skull. The surface strain field of the specimen was captured during compression and was used to derive depth-dependent moduli. These moduli were related to the morphology by optimizing parameters of a mechanical model. The tissue modulus of pure bone was also approximated as part of the modeling procedure.

S. Alexander (✉)
TKC Global Solutions LLC, 13873 Park Center Drive, Herndon, VA 20171, USA
e-mail: stephen.l.alexander18.ctr@mail.mil

C.A. Gunnarsson • A.M. DiLeonardi • T. Weerasooriya
US Army Research Laboratory, Aberdeen Proving Ground, Aberdeen, MD 21005, USA

D. Casem et al. (eds.), *Dynamic Behavior of Materials, Volume 1*, Conference Proceedings of the Society for Experimental Mechanics Series, DOI 10.1007/978-3-319-41132-3_3

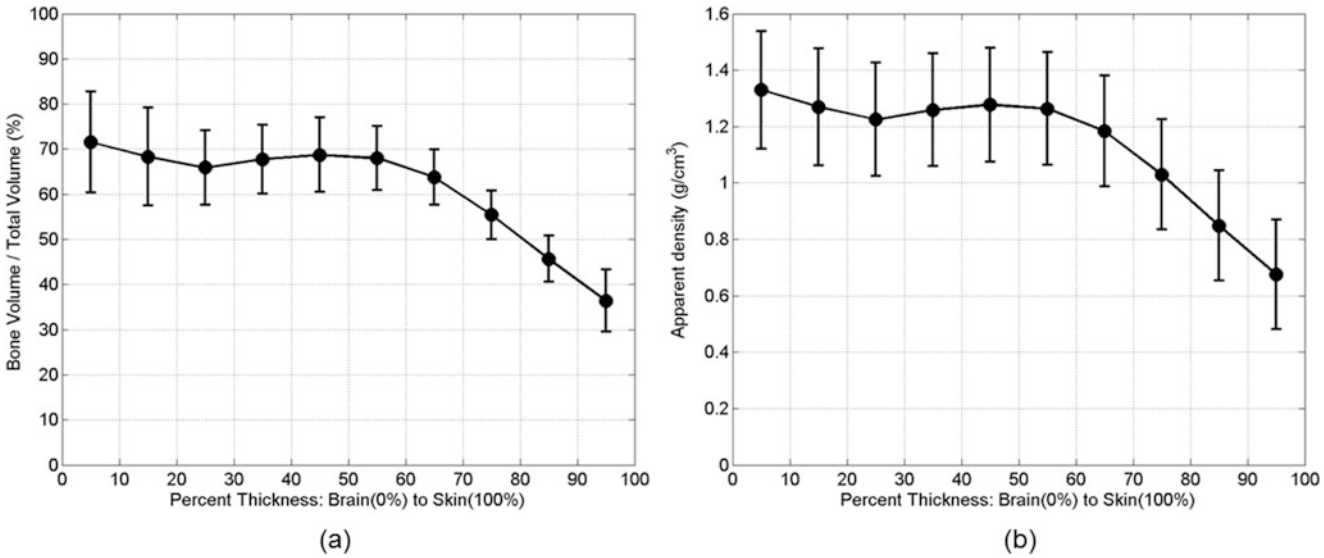

Fig. 3.1 The average bone volume fraction (**a**) and apparent density (**b**) plotted across the through-thickness axis. Percent thickness ranges from the brain-most side of the bone at 0 % to the skin-most side at 100 %. Error bars are standard deviations

3.2 Specimen Collection and Morphological Analysis

Cubical specimens (coupons), of side length 4–6 mm, were extracted from the skulls of three adolescent Göttingen minipigs (average age and weight: 26.8 weeks, 13.9 kg), following procedures previously described [6]. A total of 14 coupon specimens were imaged prior to mechanical testing using a μCT scanner (Skyscan 1172, Bruker microCT) at 62 kV and 161 mA. The size of the isotropic voxel ranged from 2.82 to 2.95 μm. The μCT image stack sampled the thickness (depth) dimension of the skull. Each image represented a cross-sectional slice of the specimen, transverse to the depth dimension and with a thickness of one voxel. The image plane will also be referred to as the transverse plane.

Morphological analysis was performed with the CTAn software, provided by the CT manufacturer. The ratio of bone area to total area of each image (depth) was assigned as the value of the bone volume fraction (f_{bv}) at that depth. The apparent density ρ_a was calculated by multiplying the bone volume fraction by the average density of pure bone, ρ_b, $\rho_a = f_{bv}\rho_b$. Figure 3.1 shows the change of bone volume fraction and apparent density as a function of depth.

The spatial orientation of the bone phase within each specimen was quantified from the μCT data using the mean intercept length (MIL) tensor [7]. In general, the principal axes of the MIL tensor correspond to the principal axes of the bone phase, averaged over the volume of interest (VOI). The degree of anisotropy (DA) was calculated as the ratio of the largest to the smallest eigenvalues of the MIL tensor.

The orientation analysis was performed on a sub-population of four specimens. The average bone orientation was measured by calculating the MIL tensor for the largest possible spherical VOI which could be extracted from the specimen. The resulting DA for the four specimens ranged from 1.20 to 1.45, much lower than the DA reported for bones from other anatomical sites. For example, Mulder et al. reported the human calcaneus to have a DA of 1.99 ± 0.29 [8]. The comparatively low DA supports the approximation of the bone phase of the skull specimens as lacking a dominant orientation.

3.3 Compression Loading and Mechanical Parameters

Unconfined, quasi-static compressive loading was applied to a sub-population of four cranial specimens (coupons). Compression was in the depth direction at an average nominal strain rate of 0.001/s. One of the surfaces perpendicular to the loading platen was speckled for digital image correlation (DIC), and a CCD camera captured the deformation of the speckled plane during loading.

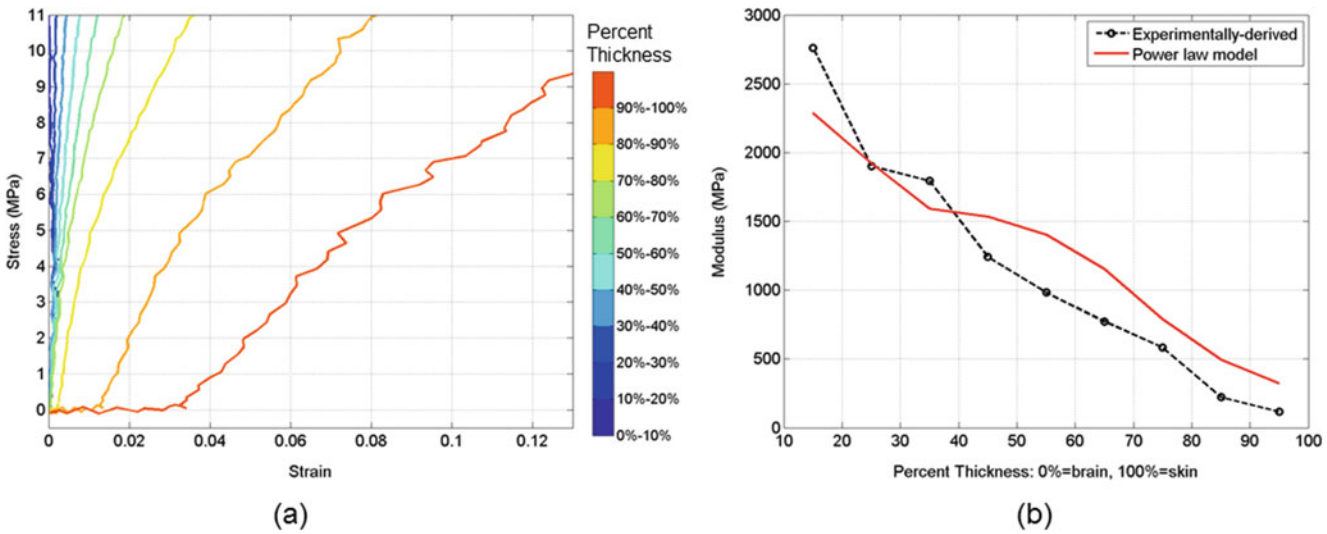

Fig. 3.2 An example of localized mechanical properties for Spec A. (**a**) The stress-strain response of each layer of Spec A, as calculated from the experimental results. Line colors correspond to the thickness percentage of the layer, as shown in the legend on right, in which a thickness of 0 % is the brain-most side and 100 % is the skin-most side. (**b**) The modulus of each layer calculated from the localized stress-strain response, together with model results

The depth-dependent stress-strain response was calculated from the experimental results of the four specimens. For each specimen, the depth dimension was divided into ten layers of equal thickness. The specimen was idealized as a parallelepiped composed of the ten layers stacked in series. The strain field over the speckled plane was calculated for each time point of the experiment. The average strain of a specific layer, ϵ^r_{yy}, was defined as the average strain over the specific $x - y$ space of the layer. The compressive stress of each layer as a function of time was calculated using the iso-stress approximation. Under this assumption, the stress in each layer was obtained directly from far-field measurements (load cell). Figure 3.2a shows an example stress-strain response for each of the layers of Spec A. The elastic moduli of each layer, E^r, were calculated from a linear regression of the initial portion of the layer's stress-strain response. These moduli were taken at layer-specific strain values roughly between $0.001 < \epsilon^r_{yy} < 0.01$ (0.1– 1% strain). Those layers for which an initial, linear stress-strain response was not discernible were not included in further analysis.

3.4 Relating Morphology and Mechanics

The extent to which the morphology of the layer could predict the layer's experimentally-derived modulus was investigated using data from the compression experiments. All morphological (e.g. density) and mechanical (e.g. strain) fields were assumed to be constant within each layer. The experimentally-measured modulus, E^r, of each layer, r, within a given specimen was assumed to be related to the tissue modulus of pure bone, E_0, scaled by a factor of the bone volume fraction of the layer,

$$E^r = E_0 (f^r_{bv})^k. \tag{3.1}$$

In Eq. 3.1, ${f_{bv}}^r$, refers to the average bone volume fraction over the spatial area of the layer r. The relationship between the apparent modulus of the porous structure and the modulus of pure bone, scaled by a power of the bone volume fraction, has been well-established [9]. However, these power-law relationships have primarily been used to relate the far-field modulus to the specimen-averaged bone volume fraction. The present methodology extends this method to calculate localized moduli within each specimen, based on spatial changes in morphology.

Equation 3.1 requires two parameters to be optimized, E_0 and the scaling parameter, k. They were optimized by fitting to the layer-specific moduli calculated from the experimental results, and the resulting relationship was

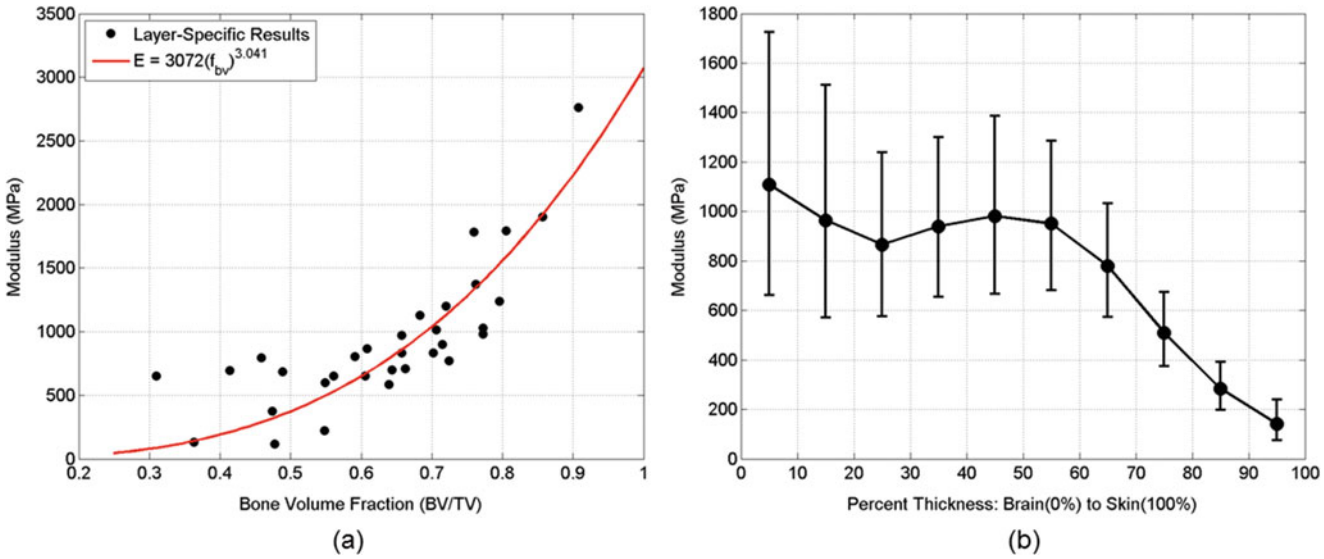

Fig. 3.3 Model results and prediction. (**a**) The modulus of each layer, calculated from the compression experiments, is plotted as a function of the layer's bone volume fraction, as measured from the μCT results. The red line is the model fit. (**b**) Model prediction for the change of modulus as a function of depth for all 14 specimens. Error bars indicate standard deviation of the bone volume fraction of each layer (Fig. 3.1a)

$$E = 3072\left(f_{bv}^{r}\right)^{3.041}. \tag{3.2}$$

Figure 3.2b shows an example of the model fit for one of the specimens, Spec A. Figure 3.3a shows the data from all specimens used in optimization, plotting the modulus of each of the layers as a function of the layer's averaged bone volume fraction.

After optimization, Eq. 3.2 was then applied to the average change of bone volume fraction as calculated for all 14 specimens, previously shown in Fig. 3.1b. Figure 3.3b shows the resulting prediction of the change of modulus with depth. The brain-surface portion of the bone was predicted to be, on average, approximately five times stiffer than the skin-surface.

3.5 Conclusions

The cranial bone morphology of the adolescent Göttingen minipig was quantified using μCT imaging with a resolution on the order of 3 μm. The volume fraction of the bone and its orientation within the skull were calculated from the images. Adolescent minipig skull specimens had denser bone near the brain, which gradually transitioned to more porous bone near the skin. This arrangement is the inverse of what has been previously reported in immature large-breed pigs and humans [3].

The compressive mechanical response of cranial bone was also measured. A relationship between localized bone volume fraction and modulus was developed using a small subset of specimens. One of the fundamental assumptions of the modeling technique was the absence of significant mechanical anisotropy. A preliminary investigation of the extent to which the structure was randomly arranged relied on MIL analysis of the μCT dataset and indicated a low degree of structural anisotropy.

The results of the isotropic model were applied to the larger group of specimens to predict the modulus-depth dependence. The model parameter corresponding to the bone tissue modulus was found to be 3.1 GPa. Researchers have previously approximated the tissue modulus of trabecular (highly porous) bone as 12 GPa, based on the range of results from experimental studies which directly measured this modulus [1]. The slightly lower value found for the minipig in this study likely arises from age effects. The isotropic model scaled the tissue modulus by the value of the bone volume fraction with an exponential factor of 3.04. This value aligns with previous studies, which show the scaling parameter to range from 2 to 3 [2].

This study was limited in the assumptions employed in the mechanical model, the small number of specimens used in parameter optimization, and the lack of an independent validation study. Perhaps most importantly, the model did not account for the spatial variation of bone orientation. Further investigation of the influence of the structural anisotropy on the mechanical results, and any conclusions as to the presence of mechanical anisotropy, would require other methods which could capture local variations in the morphology with greater precision.

Disclaimer The research reported in this document was performed in connection with contract/instrument W911-QX-14-C0016 with the U.S. Army Research Laboratory. The views and conclusions contained in this document are those of TKC Global Inc. and the U.S. Army Research Laboratory. Citation of manufacturer's or trade names does not constitute an official endorsement or approval of the use thereof. The U.S. Government is authorized to reproduce and distribute reprints for Government purposes notwithstanding any copyright notation hereon.

References

1. Gibson, L.J., Ashby, M.F.: Cellular solids: Structure and properties. Cambridge University Press, Cambridge (1997)
2. Mow, V.C., Huiskes, R.: Basic Orthopaedic Biomechanics & Mechano-Biology. Lippincott Williams & Wilkins, Philadelphia (2005)
3. Margulies, S.S., Thibault, K.L.: Infant skull and suture properties: Measurements and implications for mechanisms of pediatric brain injury. J. Biomech. Eng. **122**(4), 364–371 (2000)
4. McElhaney, J.H., Fogle, J.L., Melvin, J.W., Haynes, R.R., Roberts, V.L., Alem, N.M.: Mechanical properties of cranial bone. J. Biomech. **3**(5), 495–511 (1970)
5. Sauleau, P., Lapouble, E., Val-Laillet, D., Malbert, C.H.: The pig model in brain imaging and neurosurgery. Animal **3**(8), 1138–1151 (2009)
6. DiLeonardi, A.M., Gunnarsson, C.A., Sanborn, B., Weerasooriya, T.: Orientation dependent mechanical response and quantification of cranial bone of the Göttingen pig. In Proceedings of the Conference: SEM 2015 Annual Conference & Exposition on Experimental & Applied Mechanics, Riverside, CA (2015)
7. Harrigan, T., Mann, R.: Characterization of microstructural anisotropy in orthotropic materials using a second rank tensor. J. Mater. Sci. **19**(3), 761–767 (1984)
8. Souzanchi, M.F., Palacio-Mancheno, P., Borisov, Y.A., Cardoso, L., Cowin, S.C.: Microarchitecture and bone quality in the human calcaneus: Local variations of fabric anisotropy. J. Bone Miner. Res. **27**(12), 2562–2572 (2012)
9. Helgason, B., Perilli, E., Schileo, E., Taddei, F., Brynjólfsson, S., Viceconti, M.: Mathematical relationships between bone density and mechanical properties: A literature review. Clin. Biomech. **23**(2), 135–146 (2008)